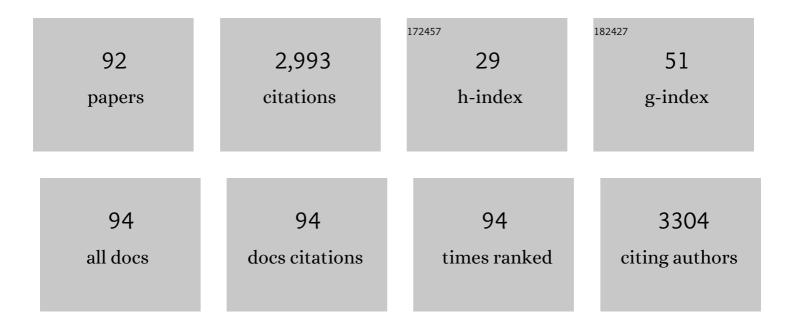
## List of Publications by Year in descending order

Source: https://exaly.com/author-pdf/1654567/publications.pdf Version: 2024-02-01



Kumli

#	Article	IF	CITATIONS
1	An efficient and stable magnetic nano-biocatalyst for biodiesel synthesis in recyclable ionic liquids. Biomass Conversion and Biorefinery, 2023, 13, 11947-11957.	4.6	1
2	Effects and behaviors of Microcystis aeruginosa in defluorination by two Al-based coagulants, AlCl3 and Al13. Chemosphere, 2022, 286, 131865.	8.2	6
3	Millimeter-Wave Active Integrated Semielliptic CPW Slot Antenna With Ultrawideband Compensation of Ball Grid Array Interconnection. IEEE Transactions on Components, Packaging and Manufacturing Technology, 2022, 12, 111-120.	2.5	4
4	Preparation of chiral aryl alcohols: a controllable enzymatic strategy <i>via</i> light-driven NAD(P)H regeneration. New Journal of Chemistry, 2022, 46, 6274-6282.	2.8	6
5	Distribution and migration of polycyclic aromatic hydrocarbons in sediment and water of the Three Gorges Reservoir. Soil Science Society of America Journal, 2022, 86, 566-578.	2.2	0
6	Multilevel Scattering Center and Deep Feature Fusion Learning Framework for SAR Target Recognition. IEEE Transactions on Geoscience and Remote Sensing, 2022, 60, 1-14.	6.3	12
7	The miR-200 Family Targeting amh Affects the Gonadal Development of Japanese Flounder. Fishes, 2022, 7, 129.	1.7	Ο
8	Stable isotope analyses of nitrogen source and preference for ammonium versus nitrate of riparian plants during the plant growing season in Taihu Lake Basin. Science of the Total Environment, 2021, 763, 143029.	8.0	18
9	A fully conjugated organic polymer via Knoevenagel condensation for fast separation of uranium. Journal of Hazardous Materials, 2021, 401, 123802.	12.4	30
10	From source to sink: Review and prospects of microplastics in wetland ecosystems. Science of the Total Environment, 2021, 758, 143633.	8.0	77
11	A novel near-infrared fluorescent sensor for zero background nitrite detection via the "covalent-assembly―principle. Food Chemistry, 2021, 341, 128254.	8.2	19
12	Evolution of membrane fouling and cleaning strategy development in municipal wastewater reclamation by nanofiltration. Environmental Technology (United Kingdom), 2021, 42, 1967-1978.	2.2	3
13	Multifunctional lipophilic purines: a coping strategy for anti-counterfeiting, lipid droplet imaging and latent fingerprint development. Materials Chemistry Frontiers, 2021, 5, 6603-6610.	5.9	11
14	Infrared and visible image fusion via octave Gaussian pyramid framework. Scientific Reports, 2021, 11, 1235.	3.3	6
15	Endogenous SO2-dependent Smad3 redox modification controls vascular remodeling. Redox Biology, 2021, 41, 101898.	9.0	22
16	Effects of polystyrene nanoplastics on extracellular polymeric substance composition of activated sludge: The role of surface functional groups. Environmental Pollution, 2021, 279, 116904.	7.5	33
17	Quantitative evaluation of the non-thermal effect in microwave induced polymer curing. RSC Advances, 2021, 11, 3740-3750.	3.6	14
18	The development and initial evaluation of referral flowchart for suspected neuroblastoma for pediatricians in nononcology clinics in China. Pediatric Blood and Cancer, 2021, 68, e28869.	1.5	0

#	Article	IF	CITATIONS
19	Sulphenylation of CypD at Cysteine 104: A Novel Mechanism by Which SO2 Inhibits Cardiomyocyte Apoptosis. Frontiers in Cell and Developmental Biology, 2021, 9, 784799.	3.7	4
20	Compensatory role of endogenous sulfur dioxide in nitric oxide deficiency-induced hypertension. Redox Biology, 2021, 48, 102192.	9.0	5
21	Differential responses of encoding-amoA nitrifiers and nir denitrifiers in activated sludge to anatase and rutile TiO2 nanoparticles: What is active functional guild in rate limiting step of nitrogen cycle?. Journal of Hazardous Materials, 2020, 384, 121388.	12.4	21
22	Multicomponent Cascade Reaction by Metal-Free Aerobic Oxidation for Synthesis of Highly Functionalized 2-Amino-4-coumarinyl-5-arylpyrroles. Journal of Organic Chemistry, 2020, 85, 327-338.	3.2	26
23	HClO/ClO <sup>–</sup> -Indicative Interpenetrating Polymer Network Hydrogels as Intelligent Bioactive Materials for Wound Healing. ACS Applied Bio Materials, 2020, 3, 37-44.	4.6	13
24	Effect of perfluorooctanesulfonate (PFOS) on the rhizosphere soil nitrogen cycling of two riparian plants. Science of the Total Environment, 2020, 741, 140494.	8.0	19
25	An environmentally benign cascade reaction of chromone-3-carboxaldehydes with ethyl 2-(pyridine-2-yl)acetate derivatives for highly site-selective synthesis of quinolizines and quinolizinium salts in water. Green Chemistry, 2020, 22, 6943-6953.	9.0	25
26	Dental follicle stem cells rescue the regenerative capacity of inflamed rat dental pulp through a paracrine pathway. Stem Cell Research and Therapy, 2020, 11, 333.	5.5	25
27	Colyliform Crystalline 2D Covalent Organic Frameworks (COFs) with Quasiâ€3D Topologies for Rapid I <sub>2</sub> Adsorption. Angewandte Chemie, 2020, 132, 22886-22894.	2.0	26
28	Colyliform Crystalline 2D Covalent Organic Frameworks (COFs) with Quasiâ€3D Topologies for Rapid I <sub>2</sub> Adsorption. Angewandte Chemie - International Edition, 2020, 59, 22697-22705.	13.8	163
29	Plant-Inspired Multifunctional Fluorescent Hydrogel: A Highly Stretchable and Recoverable Self-Healing Platform with Water-Controlled Adhesiveness for Highly Effective Antibacterial Application and Data Encryption–Decryption. ACS Applied Materials & Interfaces, 2020, 12, 57686-57694.	8.0	14
30	Effects of aging and transformation of anatase and rutile TiO2 nanoparticles on biological phosphorus removal in sequencing batch reactors and related toxic mechanisms. Journal of Hazardous Materials, 2020, 398, 123030.	12.4	17
31	Responses of freshwater biofilm formation processes (from colonization to maturity) to anatase and rutile TiO2 nanoparticles: Effects of nanoparticles aging and transformation. Water Research, 2020, 182, 115953.	11.3	21
32	Post treatment of swine anaerobic effluent by weak electric field following intermittent vacuum assisted adjustment of N:P ratio for oil-rich filamentous microalgae production. Bioresource Technology, 2020, 314, 123718.	9.6	24
33	Donor and acceptor engineering for BINOL based AIEgens with enhanced fluorescence performance. Materials Advances, 2020, 1, 61-70.	5.4	3
34	Phosphorus species in bottom sediments of the Three Gorges Reservoir during low and high water level periods. Environmental Science and Pollution Research, 2020, 27, 17923-17934.	5.3	11
35	Bio-inspired assembly in a phospholipid bilayer: effective regulation of electrostatic and hydrophobic interactions for plasma membrane specific probes. Chemical Communications, 2020, 56, 3661-3664.	4.1	9
36	Macrophage-derived sulfur dioxide is a novel inflammation regulator. Biochemical and Biophysical Research Communications, 2020, 524, 916-922.	2.1	16

#	Article	IF	CITATIONS
37	Fast Visibility Restoration Using a Single Degradation Image in Scattering Media. IEEE Photonics Journal, 2020, 12, 1-13.	2.0	5
38	A Broadband Ka-band Antenna with Asymmetric CPW Structure for package integration. , 2020, , .		0
39	Effects of sediment components and TiO2 nanoparticles on perfluorooctane sulfonate adsorption properties. Journal of Soils and Sediments, 2019, 19, 2034-2047.	3.0	8
40	Exogenic glucose as an electron donor for algal hydrogenases to promote hydrogen photoproduction by Chlorella pyrenoidosa. Bioresource Technology, 2019, 289, 121762.	9.6	17
41	Microalgae biotechnology as an attempt for bioregenerative life support systems: problems and prospects. Journal of Chemical Technology and Biotechnology, 2019, 94, 3039-3048.	3.2	17
42	High-value chemicals from Botryococcus braunii and their current applications – A review. Bioresource Technology, 2019, 291, 121911.	9.6	33
43	Microalgae-based wastewater treatment for nutrients recovery: A review. Bioresource Technology, 2019, 291, 121934.	9.6	413
44	Multicomponent Tether Catalysis Synthesis of Highly Functionalized 4-(Pyridin-2-ylmethyl)-2-aminopyrroles via Cascade Reaction Is Accompanied by Decarboxylation. Journal of Organic Chemistry, 2019, 84, 11971-11982.	3.2	18
45	Synthesis of high drug loading, reactive oxygen species and esterase dual-responsive polymeric micelles for drug delivery. RSC Advances, 2019, 9, 2371-2378.	3.6	18
46	A near-infrared water-soluble fluorescent probe for the detection of biothiols in living cells and <i>Escherichia coli</i> . Analytical Methods, 2019, 11, 821-826.	2.7	6
47	Phytotoxicity and oxidative stress of perfluorooctanesulfonate to two riparian plants: Acorus calamus and Phragmites communis. Ecotoxicology and Environmental Safety, 2019, 180, 215-226.	6.0	43
48	Differential toxicity of anatase and rutile TiO <sub>2</sub> nanoparticles to the antioxidant enzyme system and metabolic activities of freshwater biofilms based on microelectrodes and fluorescence <i>in situ</i> hybridization. Environmental Science: Nano, 2019, 6, 2626-2640.	4.3	12
49	Microbial communityâ€assisted water quality control and nutrients recovery: emerging technologies for the sustainable development of aquaponics. Journal of Chemical Technology and Biotechnology, 2019, 94, 2405-2411.	3.2	14
50	Toxicity of Three Crystalline TiO <sub>2</sub> Nanoparticles in Activated Sludge: Bacterial Cell Death Modes Differentially Weaken Sludge Dewaterability. Environmental Science & Technology, 2019, 53, 4542-4555.	10.0	70
51	Three-Component Cascade Reaction of 1,1-Enediamines, N,N-Dimethylformamide Dimethyl Acetal, and 1,3-Dicarbonyl Compounds: Selective Synthesis of Diverse 2-Aminopyridine Derivatives. ACS Omega, 2019, 4, 2863-2873.	3.5	2
52	Efficient 3D large-scale forward modeling of gravity anomaly in space-wavenumber mixing domain. , 2019, , .		0
53	Allergenicity assessment on thermally processed peanut influenced by extraction and assessment methods. Food Chemistry, 2019, 281, 130-139.	8.2	45
54	The migration and transformation behavior of heavy metals during co-liquefaction of municipal sewage sludge and lignocellulosic biomass. Bioresource Technology, 2018, 259, 156-163.	9.6	74

#	Article	IF	CITATIONS
55	Study on the formation and properties of red blood cell-like Fe <sub>3</sub> O <sub>4</sub> /TbLa <sub>3</sub> (Bim) <sub>12</sub> /PLGA composite particles. RSC Advances, 2018, 8, 12503-12516.	3.6	12
56	Structural Variation and Microrheological Properties of a Homogeneous Polysaccharide from Wheat Germ. Journal of Agricultural and Food Chemistry, 2018, 66, 2977-2987.	5.2	33
57	Dental Follicle Stem Cells Ameliorate Lipopolysaccharide-Induced Inflammation by Secreting TGF-β3 and TSP-1 to Elicit Macrophage M2 Polarization. Cellular Physiology and Biochemistry, 2018, 51, 2290-2308.	1.6	52
58	Novel easily available purine-based AIEgens with colour tunability and applications in lipid droplet imaging. Chemical Science, 2018, 9, 8969-8974.	7.4	75
59	The Increased Endogenous Sulfur Dioxide Acts as a Compensatory Mechanism for the Downregulated Endogenous Hydrogen Sulfide Pathway in the Endothelial Cell Inflammation. Frontiers in Immunology, 2018, 9, 882.	4.8	50
60	Unraveling adsorption behavior and mechanism of perfluorooctane sulfonate (PFOS) on aging aquatic sediments contaminated with engineered nano-TiO2. Environmental Science and Pollution Research, 2018, 25, 17878-17889.	5.3	6
61	Development of immunoaffinity chromatographic method for Ara h 2 isolation. Protein Expression and Purification, 2017, 131, 85-90.	1.3	1
62	Adsorption of perfluorooctane sulfonate on soils: Effects of soil characteristics and phosphate competition. Chemosphere, 2017, 168, 1383-1388.	8.2	41
63	Ara h 2 cross-linking catalyzed by MTGase decreases its allergenicity. Food and Function, 2017, 8, 1195-1203.	4.6	15
64	Fractions and spatial distributions of agricultural riparian soil phosphorus in a small river basin of Taihu area, China. Chemical Speciation and Bioavailability, 2017, 29, 33-41.	2.0	4
65	Effects of carbon nanotubes on phosphorus adsorption behaviors on aquatic sediments. Ecotoxicology and Environmental Safety, 2017, 142, 230-236.	6.0	8
66	A tumor-specific and mitochondria-targeted fluorescent probe for real-time sensing of hypochlorite in living cells. Chemical Communications, 2017, 53, 5539-5541.	4.1	115
67	Perfluorooctane sulfonate adsorption on powder activated carbon: Effect of phosphate (P) competition, pH, and temperature. Chemosphere, 2017, 182, 215-222.	8.2	46
68	Toxic effects of three crystalline phases of TiO2 nanoparticles on extracellular polymeric substances in freshwater biofilms. Bioresource Technology, 2017, 241, 276-283.	9.6	47
69	Co-adsorption of perfluorooctane sulfonate and phosphate on boehmite: Influence of temperature, phosphate initial concentration and pH. Ecotoxicology and Environmental Safety, 2017, 137, 71-77.	6.0	31
70	Water sources of riparian plants during a rainy season in Taihu Lake Basin, China: a stable isotope study. Chemical Speciation and Bioavailability, 2017, 29, 153-160.	2.0	6
71	Crystalline phase-dependent eco-toxicity of titania nanoparticles toÂfreshwater biofilms. Environmental Pollution, 2017, 231, 1433-1441.	7.5	15
72	Sulphur dioxide suppresses inflammatory response by sulphenylating NF-κB p65 at Cys38 in a rat model of acute lung injury. Clinical Science, 2017, 131, 2655-2670.	4.3	36

#	Article	IF	CITATIONS
73	Exploration of a mechanism for the production of highly unsaturated fatty acids in Scenedesmus sp. at low temperature grown on oil crop residue based medium. Bioresource Technology, 2017, 244, 542-551.	9.6	44
74	Endogenous sulfur dioxide alleviates collagen remodeling via inhibiting TGF-β/Smad pathway in vascular smooth muscle cells. Scientific Reports, 2016, 6, 19503.	3.3	33
75	Downregulated endogenous sulfur dioxide/aspartate aminotransferase pathway is involved in angiotensin II-stimulated cardiomyocyte autophagy and myocardial hypertrophy in mice. International Journal of Cardiology, 2016, 225, 392-401.	1.7	31
76	Electrospraying magnetic-fluorescent bifunctional Janus PLGA microspheres with dual rare earth ions fluorescent-labeling drugs. RSC Advances, 2016, 6, 99034-99043.	3.6	14
77	Novel mitochondria-targeted, nitrogen mustard-based DNA alkylation agents with near infrared fluorescence emission. Talanta, 2016, 161, 888-893.	5.5	13
78	Development of a mitochondria-targeted fluorescent probe for hydrazine monitoring in living cells. RSC Advances, 2016, 6, 111016-111019.	3.6	34
79	Red emission fluorescent probes for visualization of monoamine oxidase in living cells. Scientific Reports, 2016, 6, 31217.	3.3	24
80	A water-soluble and fast-response mitochondria-targeted fluorescent probe for colorimetric and ratiometric sensing of endogenously generated SO <sub>2</sub> derivatives in living cells. Chemical Communications, 2016, 52, 3430-3433.	4.1	114
81	Novel Tumor-Specific and Mitochondria-Targeted near-Infrared-Emission Fluorescent Probe for SO <sub>2</sub> Derivatives in Living Cells. ACS Sensors, 2016, 1, 166-172.	7.8	104
82	Utilization of municipal solid and liquid wastes for bioenergy and bioproducts production. Bioresource Technology, 2016, 215, 163-172.	9.6	141
83	A single design strategy for dual sensitive pH probe with a suitable range to map pH in living cells. Scientific Reports, 2015, 5, 15540.	3.3	16
84	Long-Term Changes in the Water Quality and Macroinvertebrate Communities of a Subtropical River in South China. Water (Switzerland), 2015, 7, 63-80.	2.7	15
85	The dicyclen–TPE zinc complex as a novel fluorescent ensemble for nanomolar pyrophosphate sensing in 100% aqueous solution. Organic Chemistry Frontiers, 2014, 1, 1276-1279.	4.5	12
86	Rhodamine-based lysosome-targeted fluorescence probes: high pH sensitivity and their imaging application in living cells. RSC Advances, 2014, 4, 33975-33980.	3.6	20
87	A Rapid Surface-Enhanced Raman Scattering Method for the Determination of Trace Hg2+ Using Rhodamine 6G-Aggregated Nanosilver as Probe. Plasmonics, 2012, 7, 461-468.	3.4	18
88	Oriented Smoothness Aided Harmonic Gradient Vector Flow for Active Contours. , 2009, , .		3
89	Immobilization cyclen copper (II) on merrifield resin: Efficient oxidative cleavage of plasmid DNA. Journal of Applied Polymer Science, 2009, 111, 2485-2492.	2.6	10
90	Lipase-catalysed direct Mannich reaction in water: utilization of biocatalytic promiscuity for C–C bond formation in a "one-pot―synthesis. Green Chemistry, 2009, 11, 777.	9.0	167

#	Article	IF	Citations
91	Lipase-catalysed decarboxylative aldol reaction and decarboxylative Knoevenagel reaction. Green Chemistry, 2009, 11, 1933.	9.0	80
92	AMS Radiocarbon Dating of Tianma-Qucun Site in Shanxi, China. Radiocarbon, 2001, 43, 1109-1114.	1.8	8